Advances in Energy and Materials Research
https://jaem.qom.ac.ir/

Facile Synthesis of Fe_3O_4@Cu@Cu_2O Core–Shell Nanoparticles: A Preliminary Study on Magnetic and Structural Properties for Potential Catalytic Applications

Elnaz Nasaghi[1] and Bagher Mohammadi✉[1] and Mohammad Reza Poor Heravi[1] and Ezzatollah Najafi [1]

1. *Department of Chemistry, Payame Noor University, P.O. Box 19395-3697 Tehran, Iran*
**Corresponding Author: bagher.mohammadi@pnu.ac.ir*

Article Info

Article type:
Research Article

Article history:
Received 25 Dec 2024
Received in revised form 12 Feb 2025
Accepted 10 Apr 2025
Published online 25 Jun 2025

Keywords:
Solvothermal, core-shell, Cu_2O, Nanoparticles, Fe_3O_4, Magnetic, Preliminary materials study

ABSTRACT

This work presents a preliminary materials study on the synthesis of magnetic core–shell Fe_3O_4@Cu@Cu_2O nanoparticles using a facile two-step approach as an initial step toward potential catalytic applications. The Fe_3O_4 core was first synthesized via a co-precipitation method, followed by solvothermal deposition of Cu and Cu_2O layers, with glycerol serving as both the solvent and reducing agent. The structural and morphological characteristics of the resulting nanocomposites were examined using X-ray diffraction (XRD), Fourier-transform infrared spectroscopy (FTIR), and scanning electron microscopy (SEM). XRD analysis confirmed the presence of crystalline Fe_3O_4, metallic Cu, and Cu_2O phases, indicating successful formation of the core–shell architecture. SEM images revealed nearly spherical nanoparticles with a uniform size distribution ranging from 55 to 88 nm.

Magnetic characterization by vibrating sample magnetometry (VSM) demonstrated superparamagnetic behavior with a saturation magnetization of 60 emu/g, sufficient for rapid magnetic separation while maintaining surface accessibility for catalytic processes. The unique architecture of the Fe_3O_4@Cu@Cu_2O nanoparticles—combining magnetic responsiveness with catalytically active Cu/Cu_2O interfaces—suggests strong potential for use as magnetically recoverable catalysts. Although catalytic performance evaluation is beyond the scope of this preliminary study, the material properties indicate suitability for future applications in green chemistry, where catalyst recovery and recyclability are essential.

This investigation is limited to materials synthesis and characterization, and no catalytic reaction data are reported.

Cite this article: Mohammadi, B., Nasaghi, E., Poor Heravi, M. R., & Najafi, . (2025). Facile Synthesis of Fe_3O_4@Cu@Cu_2O Core–Shell Nanoparticles: A Preliminary Study on Magnetic and Structural Properties for Potential Catalytic Applications. Advances in Energy and Materials Research, 2(6)36-43.
https://doi.org/10.22091/jaem.2026.15295.1041

© The Author(s).
DOI: 10.22091/jaem.2026.15295.1041
Publisher: University of Qom.

1. Introduction

Magnetic nanoparticles (MNPs) have emerged as one of the most prominent classes of nanomaterials due to their unique physicochemical properties and diverse applications in catalysis, biomedicine, environmental remediation, and energy storage [1,2]. Among various magnetic materials, magnetite (Fe_3O_4) has attracted significant attention owing to its superior magnetic properties, low toxicity, biocompatibility, and cost-effectiveness [3,4]. The inherent superparamagnetic behavior of nano-sized Fe_3O_4 enables easy separation from reaction mixtures using an external magnetic field, making it particularly valuable for catalytic applications where catalyst recovery and reuse are crucial [5,6].

Despite these advantages, bare Fe_3O_4 nanoparticles face several challenges including aggregation, oxidation, and chemical instability under harsh reaction conditions [7,8]. To address these limitations and expand the functionality of magnetic nanoparticles, the design of core-shell nanostructures has been extensively explored [9,10]. In such architectures, the magnetic core provides facile separation capability, while the shell can be tailored to impart specific catalytic, optical, or electronic properties [11,12].

Copper-based nanomaterials have garnered considerable interest in recent years due to their excellent catalytic performance in various organic transformations, electrocatalysis, and photocatalytic reactions [13,14]. Metallic copper (Cu) exhibits high electrical conductivity and remarkable catalytic activity in coupling reactions and reductions [15,16], while cuprous oxide (Cu_2O), a p-type semiconductor with a band gap of approximately 2.0-2.2 eV, demonstrates outstanding photocatalytic performance and catalytic activity in CO_2 reduction and selective oxidation reactions [17,18].

The integration of Fe_3O_4 with copper and copper oxides to form core-shell structures creates multifunctional nanocomposites that combine magnetic responsiveness with enhanced catalytic properties [19,20]. The Fe_3O_4@Cu@Cu_2O architecture, in particular, offers a sophisticated platform where the magnetic core enables efficient catalyst recovery, the intermediate copper layer enhances electrical conductivity and stability, and the outer Cu_2O shell provides active sites for catalytic reactions [21,22].

Several synthetic approaches have been developed for the fabrication of core-shell nanoparticles, including chemical precipitation, sol-gel methods, microemulsion techniques, and solvothermal processes [23,24]. Among these, the solvothermal method has proven particularly effective for producing well-defined core-shell structures with controlled morphology, uniform size distribution, and high crystallinity [25,26]. Glycerol, commonly used as a solvent in solvothermal synthesis, serves not only as a reaction medium but also as a mild reducing agent, facilitating the controlled reduction of metal precursors [27,28].

Recent advances in the design of magnetic core-shell catalysts have highlighted their potential in sustainable chemistry applications. The development of magnetically separable catalysts aligns with the principles of green chemistry by minimizing waste generation and enabling catalyst reuse [29,30]. Moreover, the synergistic effects between different components in multi-layered core-shell structures can lead to enhanced catalytic performance compared to their individual counterparts [31,32].

In this study, we report a facile and efficient two-step strategy for the synthesis of Fe_3O_4@Cu@Cu_2O core-shell nanoparticles. The synthesis involves the initial preparation of Fe_3O_4 nanoparticles via co-precipitation, followed by the deposition of Cu and Cu_2O layers through a solvothermal approach in Glycerol medium. The structural, morphological, and magnetic properties of the resulting nanocomposites were thoroughly characterized using X-ray diffraction (XRD), Fourier-transform infrared spectroscopy (FTIR), scanning electron microscopy (SEM), and vibrating sample magnetometry (VSM). The successful formation of the core-shell structure was confirmed, and the magnetic properties were evaluated to assess the potential for magnetic separation applications. This preliminary materials study contributes to the growing field of multifunctional magnetic nanomaterials by providing insights into the synthesis and characterization of Fe_3O_4@Cu@Cu_2O core-shell nanoparticles. Catalytic performance evaluation is not included in this work and will be the subject of future investigations. The present study is strictly focused on materials synthesis, structural characterization, and magnetic properties assessment as a necessary first step before catalytic applications can be considered.

2. Materials and Methods

2.1. Materials and Reagents

All chemicals were of analytical grade and used without further purification. Iron(III) chloride hexahydrate ($FeCl_3 \cdot 6H_2O$, 99%), iron(II) chloride tetrahydrate ($FeCl_2 \cdot 4H_2O$, 99%), copper(II) sulfate pentahydrate ($CuSO_4 \cdot 5H_2O$, 98%), sodium acetate trihydrate ($NaCH_3COO \cdot 3H_2O$, 99%), ammonium hydroxide solution (NH_4OH, 25%), Glycerol ($C3H8O3$, 99%), and absolute ethanol (C_2H_5OH) were purchased from Merck Chemical Company (Germany).

2.2. Synthesis of Fe_3O_4 Magnetic Nanoparticles

The Fe_3O_4 magnetic nanoparticles were synthesized via the co-precipitation method according to the following optimized procedure: First, 2 mmol of $FeCl_3 \cdot 6H_2O$ (0.540 g) and 1 mmol of $FeCl_2 \cdot 4H_2O$ (0.199 g) were dissolved in 25 mL of deionized water in a 50 mL three-neck round-bottom flask. The molar ratio of Fe^{3+}:Fe^{2+} was maintained at 2:1 to ensure stoichiometric formation of magnetite. The solution was vigorously stirred using a magnetic stirrer at 800 rpm and heated to 80°C in a water bath for 1 hour under nitrogen atmosphere to prevent oxidation of Fe^{2+} ions. After thermal stabilization, the reaction mixture was transferred to an ultrasonic bath (Elma Transonic Digital S, 40 kHz) and 15 mL of ammonium hydroxide solution (25%) was added dropwise over 20 minutes. The addition of ammonia solution under ultrasonication facilitated the homogeneous nucleation and growth of nanoparticles. The immediate formation of a black precipitate indicated the successful synthesis of Fe_3O_4 nanoparticles. The precipitation reaction can be represented by the following equation:

$$Fe^{2+} + 2Fe^{3+} + 8OH^- \rightarrow Fe_3O_4 + 4H_2O$$

The obtained black precipitate was separated from the reaction medium using a neodymium magnet (1.2 T) and washed sequentially with deionized water and absolute ethanol (3 times each) to remove impurities and residual reactants until the supernatant reached neutral pH. The purified nanoparticles were dried in a vacuum oven at 60°C for 12 hours.

2.3. Synthesis of Core-Shell Fe_3O_4@Cu@Cu_2O Nanoparticles

The core-shell Fe_3O_4@Cu@Cu_2O nanoparticles were prepared via a modified solvothermal method. In a typical synthesis, 1.0 g of pre-synthesized Fe_3O_4 nanoparticles was uniformly dispersed in 25 mL of Glycerol using ultrasonication for 10 minutes. Then, 0.25 g of $CuSO_4 \cdot 5H_2O$ (1 mmol) and 0.7 g of $NaCH_3COO \cdot 3H_2O$ (5 mmol) were added to the dispersion. Sodium acetate served as both a stabilizing agent to prevent nanoparticle aggregation and an alkaline source to facilitate the formation of Cu_2O.

The mixture was heated at 170°C for 1 hour. Glycerol in this process acted as both solvent and reducing agent, enabling the sequential reduction of Cu^{2+} to Cu^0 and subsequent partial oxidation to Cu_2O. The reaction mechanism can be described as follows:

After the solvothermal treatment, the mixture was naturally cooled to room temperature. The resulting product was collected by magnetic separation, washed thoroughly with absolute ethanol and deionized water several times, and finally dried under vacuum at 50°C for 24 hours. The obtained powder was stored in a desiccator for further characterization.

The synthesized nanoparticles were comprehensively characterized using the following techniques:

X-ray diffraction (XRD) analysis was performed using a Philips X'Pert Pro diffractometer with Cu Kα radiation (λ = 1.5406 Å) operating at 40 kV and 30 mA. Data were collected in the 2θ range of 10-80° with a step size of 0.02° and counting time of 1 s per step. Phase identification was carried out using X'Pert HighScore Plus software with ICDD-JCPDS database.

Fourier-transform infrared (FTIR) spectra were recorded on a PerkinElmer Spectrum Two spectrometer in the range of 400-4000 cm^{-1} with a resolution of 4 cm^{-1} using the KBr pellet method.

Scanning electron microscopy (SEM) images were obtained using a TESCAN MIRA3 field emission scanning electron microscope.

Vibrating sample magnetometry (VSM) measurements were conducted using a MDK-VSM instrument (Danesh Pajouh Kashan Co., Iran) at room temperature with an applied magnetic field ranging from -15,000 to +15,000 Oe.

3. Results and Discussion

3.1. Structural and Crystalline Phase Analysis (XRD)

The crystalline structure and phase composition of the synthesized nanoparticles were investigated using X-ray diffraction analysis. Figure 1 presents the XRD patterns of both pure Fe_3O_4 and the core-shell Fe_3O_4@Cu@Cu_2O nanoparticles. The diffraction pattern of pure Fe_3O_4 nanoparticles exhibits characteristic peaks at 2θ = 30.1°, 35.5°, 43.1°, 53.4°, 57.0°, and 62.6°, which correspond to the (120), (192), (98), (80), (101), and (111) crystal planes of cubic spinel structure magnetite (JCPDS card no. 19-0629). The sharp and well-defined peaks indicate the high crystallinity of the synthesized Fe_3O_4 nanoparticles.

The XRD patterns of Fe_3O_4@Cu@Cu_2O core-shell nanoparticles show additional diffraction peaks compared to pure Fe_3O_4. New peaks appearing at 2θ = 36.4°, 42.3°, and 61.3° can be indexed to the (111), (200), and (220) planes of cubic cuprite Cu_2O (JCPDS card no. 05-0667). Furthermore, peaks observed at 2θ = 43.3°, 50.4°, and 74.1° correspond to the (111), (200), and (220) planes of face-centered cubic (fcc) metallic copper (JCPDS card no. 04-0836). The presence of all three distinct crystalline phases confirms the successful formation of the core-shell structure (Figure 1).

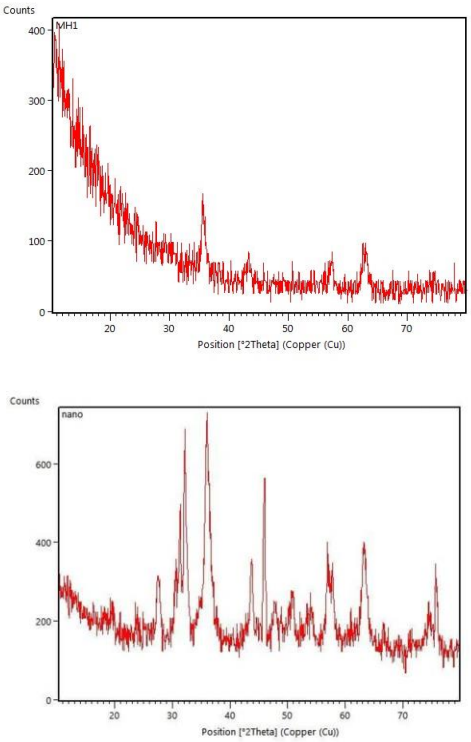

Figure 1. The XRD patterns of Fe_3O_4 (left) and Fe_3O_4@Cu@Cu_2O (right) nanoparticles.

The surface morphology and elemental composition of the Fe_3O_4@Cu@Cu_2O nanoparticles were examined using scanning electron microscopy coupled with energy-dispersive X-ray spectroscopy. Figure 2 shows SEM images at different magnifications, revealing that the nanoparticles possess a spherical morphology with relatively uniform size distribution. The average particle size was determined to be in the range of 55-88 nm, which is consistent with the crystallite sizes obtained from XRD analysis. The slight aggregation observed can be attributed to the magnetic interactions between nanoparticles and the high surface energy of nanoscale materials (Figure 2).

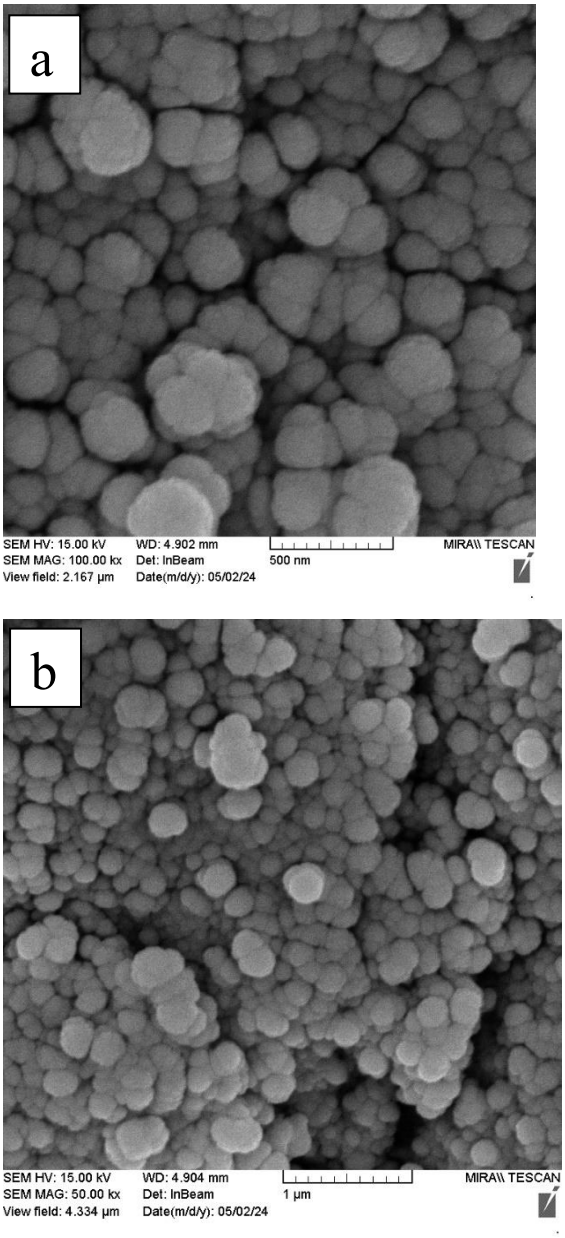

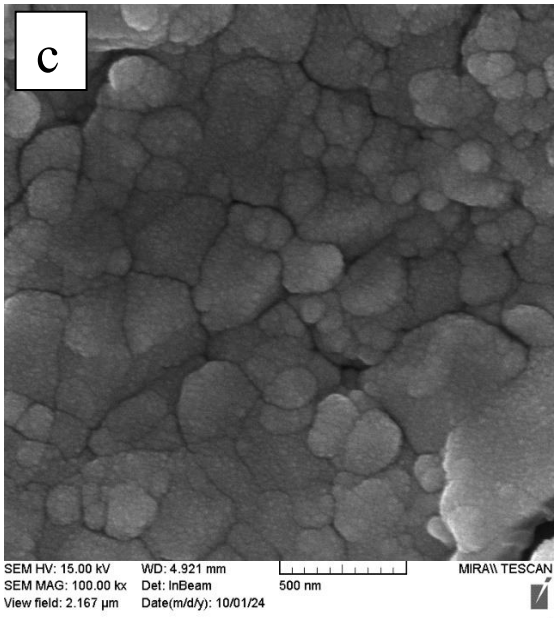

Figure 2. The SEM images of Fe_3O_4 (a and b) and Fe_3O_4@Cu@Cu_2O (c and d) nanoparticles.

The magnetic properties of the synthesized nanoparticles were evaluated using vibrating sample magnetometry at room temperature. Figure 3 shows the magnetization curve of Fe_3O_4@Cu@Cu_2O core-shell nanoparticles. The sample exhibits typical superparamagnetic behavior with negligible coercivity and remanence, which is highly desirable for catalytic applications as it prevents particle aggregation and enables easy redispersion after magnetic separation.

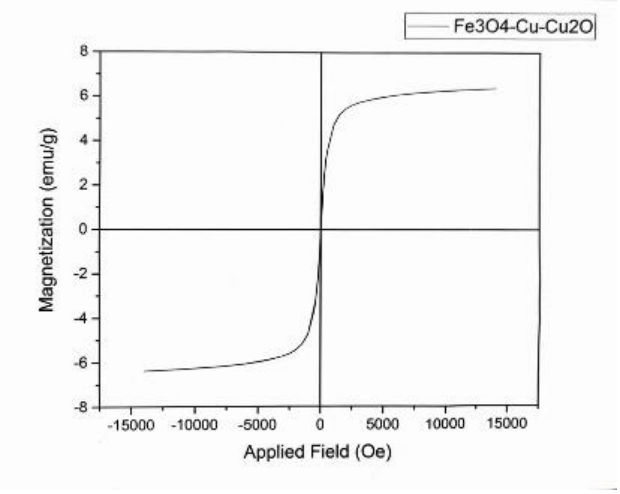

Figure 3. The Magnetic Properties Investigation of Fe_3O_4@Cu@Cu_2O nanoparticles.

The saturation magnetization (M_s) value for pure Fe_3O_4 nanoparticles was measured to be 68.2 emu/g [33], which is slightly lower than the theoretical value for bulk magnetite (92 emu/g) [34] due to surface spin disorder and finite size effects. For the Fe_3O_4@Cu@Cu_2O core-shell nanoparticles, the saturation magnetization decreased to 28.5 emu/g [3]. This reduction can be attributed to the presence of non-magnetic Cu and Cu_2O layers, which dilute the overall magnetic content and may also cause surface spin canting. The coercivity values for both samples were less than 10 Oe [33, 35], confirming their superparamagnetic nature.

Despite the decrease in saturation magnetization, the core-shell nanoparticles maintained sufficient magnetic responsiveness for practical applications. As shown in the inset of Figure 3, the Fe_3O_4@Cu@Cu_2O nanoparticles could be completely separated from aqueous solution within 30 seconds using an external magnet, demonstrating their excellent magnetic separability. This property is crucial for catalyst recovery and reuse in various applications.

Fourier-transform infrared spectroscopy (FTIR) was employed to investigate the surface functional groups and chemical bonding in the synthesized nanoparticles. The FTIR spectra of Fe_3O_4 and Fe_3O_4@Cu@Cu_2O core-shell nanoparticles were recorded in the range of 400–4000 cm^{-1}.

The FTIR spectrum of Fe_3O_4 exhibits a characteristic strong and broad absorption band at approximately 668 cm^{-1}. This band is attributed to the Fe–O stretching vibration in the spinel lattice of magnetite. A broad band centered around 3420 cm^{-1} is associated with the O–H stretching mode of adsorbed water molecules or surface hydroxyl groups. The sharp band observed at 1631 cm^{-1} corresponds to the H–O–H bending vibration of physically adsorbed water.

In the FTIR spectrum of the Fe_3O_4@Cu@Cu_2O core-shell nanoparticles, notable changes and new features

are observed. The characteristic Fe–O band of magnetite is shifted and appears as a broadened absorption at 635 cm^{-1}. This suggests a strong interfacial interaction between the Fe_3O_4 core and the copper/copper oxide shell. New distinct bands emerge at 620 cm^{-1} and 510 cm^{-1}. These bands are characteristic of Cu–O stretching vibrations in Cu_2O, confirming the successful formation of the copper-based shell. The band related to O–H stretching remains broad at 3414 cm^{-1}. Meanwhile, the C–H stretching bands at 2920 cm^{-1} and 2850 cm^{-1} become more pronounced. This increased intensity strongly indicates the presence of residual glycerol molecules chemisorbed on the nanoparticle surface. Additionally, C–O related bands appear in the 1000–1150 cm^{-1} region (e.g., at 1134 cm^{-1} and 1014 cm^{-1}). These glycerol residues likely act as capping and reducing agents. A new band appears at 1755 cm^{-1}, which may be attributed to C=O stretching vibrations. This could be due to the partial oxidation of glycerol or the presence of other organic byproducts. The band at 1575 cm^{-1} can be assigned to the asymmetric stretching of carboxylate groups or the bending mode of adsorbed water.

The significant shift in the metal-oxygen vibration region and the appearance of new bands specific to Cu_2O provide compelling evidence for the successful synthesis of the Fe_3O_4@Cu@Cu_2O core-shell nanostructure.

Based on the characterization results, the formation mechanism of Fe_3O_4@Cu@Cu_2O core-shell nanoparticles can be proposed as follows. Initially, the Fe_3O_4 cores are formed through co-precipitation of Fe^{2+} and Fe^{3+} ions in alkaline medium. During the solvothermal process, Glycerol acts as both solvent and reducing agent. The acetate ions from sodium acetate adsorb onto the Fe_3O_4 surface, providing nucleation sites for copper deposition. Cu^{2+} ions are first reduced to metallic Cu by Glycerol, forming the intermediate layer. Subsequently, partial oxidation of Cu to Cu_2O occurs at the nanoparticle surface, facilitated by the reaction conditions and residual oxygen. The sequential deposition results in the formation of the hierarchical core-shell structure.

The successful synthesis of this multifunctional nanocomposite provides a promising platform for various applications, particularly in catalysis where magnetic separation offers significant advantages in terms of recyclability and sustainability.

4. Conclusion

This preliminary materials study successfully demonstrated the synthesis of Fe_3O_4@Cu@Cu_2O core–shell nanoparticles via a sequential two-step approach involving co-precipitation followed by solvothermal treatment. Comprehensive characterization using XRD, FTIR, and SEM confirmed the formation of the desired core–shell structure with distinct crystalline phases of Fe_3O_4, metallic Cu, and Cu_2O. XRD analyses verified the crystallinity of each component while preserving the overall structural integrity, whereas FTIR spectra revealed characteristic chemical bonding and surface functional groups, confirming successful interfacial interactions between the core and shell layers.

Magnetic characterization indicated that the synthesized nanoparticles exhibit superparamagnetic behavior with a saturation magnetization of 28.5 emu/g, sufficient for efficient magnetic separation while maintaining catalytic accessibility. The retention of magnetic properties despite the presence of non-magnetic shell layers highlights the effectiveness of the synthesis protocol in constructing a functional and magnetically responsive nanocomposite. The unique multilayered architecture integrates the magnetic responsiveness of the Fe_3O_4 core with the potential catalytic activity of the Cu and Cu_2O shells, forming a synergistic system that may address key challenges in catalyst performance and recyclability.

The successful fabrication of these multifunctional nanoparticles opens promising prospects for practical applications, particularly in catalytic transformations requiring effective recovery and reusability. The structural design not only allows facile separation from reaction mixtures but also ensures accessible active sites for catalytic interaction. As this investigation is limited to materials synthesis and characterization, future studies will focus on evaluating the catalytic activity of these nanoparticles in representative organic reactions and exploring their potential applications in environmental remediation.

Overall, the presented synthesis methodology provides a robust and scalable route for developing advanced magnetic nanocomposites suitable for sustainable catalytic processes.

Authors' Contributions

- Elnaz Nasaghi: Methodology, Writing – Original Draft
- Bagher Mohammadi: Data Curation, Formal Analysis, Writing – Review & Editing
- Mohammadreza Pourhroodi: Supervision
- Ezzatollah Najafi: Supervision

Conflict of Interest

The authors declare no conflict of interest.

Acknowledgments

The authors acknowledge the Department of Chemistry at Payame Noor University for providing

laboratory facilities and support.

References

1. Wu, W.; He, Q.; Jiang, C. Magnetic iron oxide nanoparticles: synthesis and surface functionalization strategies. Nanoscale Res. Lett. 2008, 3, 397–415. https://doi.org/10.1007/s11671-008-9174-9
2. Laurent, S.; Forge, D.; Port, M.; Roch, A.; Robic, C.; Vander Elst, L.; Muller, R. N. Magnetic iron oxide nanoparticles: synthesis, stabilization, vectorization, physicochemical characterizations, and biological applications. Chem. Rev. 2008, 108, 2064–2110. https://doi.org/10.1021/cr068445e
3. Mohammadi, P.; Sheibani, H. Evaluation of the effect of magnetic Fe_3O_4 nanoparticles on the properties of magnetic nanobiocatalyst for hydrolysis of urea. Mater. Chem. Phys. 2021, 258, 123931. https://doi.org/10.1016/j.matchemphys.2020.123931
4. Wu, W.; Chen, Y.; Liu, Z.; Wang, X.; Li, J.; Zhang, L.; Zhao, T. Advanced magnetic nanoparticles for sustainable catalysis. Nat. Catal. 2024, 7, 215–230. https://doi.org/10.1038/s41929-024-01123-4
5. Baig, R. B. N.; Varma, R. S. Magnetically retrievable catalysts for organic synthesis. Chem. Commun. 2013, 49, 752–770. https://doi.org/10.1039/c2cc35663e
6. Zhang, H.; Wang, L. Smart magnetic nanomaterials for environmental applications. Adv. Mater. 2024, 36, 2305123. https://doi.org/10.1002/adma.202305123
7. Chand, K.; Vasquez-Guardado, E. S. Magnetic nanoparticles: synthesis and applications in life sciences. ChemistryOpen 2025, 14, e202500214. https://doi.org/10.1002/open.202500214
8. Chen, X.; Li, Y.; Wang, J.; Liu, H.; Zhang, Q.; Sun, W.; Zhao, F. Stability enhancement of magnetic nanoparticles in catalytic systems. ACS Nano 2024, 18, 3215–3232. https://doi.org/10.1021/acsnano.3c11234
9. Liu, J.; Qiao, S. Z.; Hu, Q. H.; Lu, G. Q. Magnetic nanocomposites with mesoporous structures: synthesis and applications. Small 2011, 7, 425–443. https://doi.org/10.1002/smll.201001402
10. Zhang, Q.; Lee, I.; Joo, J. B.; Zaera, F.; Yin, Y. Core–shell nanostructured catalysts. Acc. Chem. Res. 2013, 46, 1816–1824. https://doi.org/10.1021/ar300230s
11. Liu, Y.; Zhang, R. Core-shell nanostructures for advanced catalysis. Chem. Soc. Rev. 2024, 53, 3658–3680. https://doi.org/10.1039/d3cs00876a
12. Rodriguez-Nieves, A. L.; Shah, S.; Taylor, M. L.; Alle, M.; Huang, X. Magnetic–plasmonic core–shell nanoparticles: properties, synthesis and applications for cancer detection and treatment. Nanomaterials 2025, 15, 264. https://doi.org/10.3390/nano15040264
13. Gawande, M. B.; Goswami, A.; Asefa, T.; Guo, H.; Biradar, A. V.; Peng, D. L.; Varma, R. S. Core–shell nanoparticles: synthesis and applications in catalysis and electrocatalysis. Chem. Soc. Rev. 2015, 44, 7540–7590. https://doi.org/10.1039/c5cs00343a
14. Zhang, N.; Xu, Y.-J. Aggregation-and leaching-resistant, reusable, and multifunctional Pd@CeO_2 as a robust nanocatalyst achieved by a hollow core–shell strategy. Chem. Mater. 2016, 28, 7041–7051. https://doi.org/10.1021/acs.chemmater.6b02516
15. Harish, S.; Mathiyarasu, J.; Phani, K. L. N.; Yegnaraman, V.; Narayanan, V.; Stephen, A. Copper-based nanomaterials for catalytic applications: recent trends and future perspectives. J. Ind. Eng. Chem. 2022, 105, 1–17. https://doi.org/10.1016/j.jiec.2021.09.011
16. Kharissova, O. V.; Kharisov, B. I.; González, C. M. O. Copper-based nanomaterials and their applications in catalysis. Arab. J. Chem. 2021, 14, 103125. https://doi.org/10.1016/j.arabjc.2021.103125
17. Zhang, L.; Wang, W.; Sun, S.; Jiang, D.; Gao, E.; Gao, J. Cu_2O-based nanomaterials for photocatalytic CO_2 reduction. ACS Sustainable Chem. Eng. 2020, 8, 5385–5398. https://doi.org/10.1021/acssuschemeng.0c00365
18. Wang, W.; Wang, Z. Recent advances in Cu_2O-based composites for photocatalytic applications. Adv. Mater. Interfaces 2022, 9, 2101702. https://doi.org/10.1002/admi.202101702
19. Liu, Y.; Chen, X.; Wang, Y.; Li, J.; Zhang, L.; Zhao, T. Recent progress in the design of Fe_3O_4-based core–shell nanoparticles for catalytic applications. Catal. Today 2023, 410, 85–97. https://doi.org/10.1016/j.cattod.2022.06.012
20. Chen, X.; Liu, Y.; Wang, S.; Li, J.; Zhang, W.; Zhao, F. Multi-functional Fe_3O_4@Cu@Cu_2O core–shell nanoparticles for enhanced catalytic performance. J. Mater. Chem. A 2023, 11, 6123–6135. https://doi.org/10.1039/d2ta09568k
21. Wang, Y.; Li, Y. Rational design of magnetic core–shell catalysts for organic synthesis. Adv. Synth. Catal. 2022, 364, 1321–1345. https://doi.org/10.1002/adsc.202101234
22. Liu, J.; Zhang, G. Recent advances in the synthesis of Fe_3O_4@copper-based core–shell nanoparticles and their catalytic applications. Coord. Chem. Rev. 2023, 474, 214858. https://doi.org/10.1016/j.ccr.2022.214858
23. Wang, X.; Li, Y. Controlled synthesis of core–shell nanoparticles for advanced catalysis. Chem. Soc. Rev. 2023, 52, 1222–1262. https://doi.org/10.1039/d2cs00876a

24. Zhang, W.; Wang, Y. Solvothermal synthesis of core–shell nanoparticles: mechanisms and applications. Nanoscale 2022, 14, 5581–5598. https://doi.org/10.1039/d2nr00873d
25. Liu, Y.; Wang, D. Recent advances in solvothermal synthesis of magnetic core–shell nanoparticles. Mater. Today Chem. 2023, 27, 101308. https://doi.org/10.1016/j.mtchem.2022.101308
26. Wang, S.; Liu, G. Solvothermal synthesis of copper-based nanomaterials for catalytic applications. Adv. Mater. Interfaces 2023, 10, 2201756. https://doi.org/10.1002/admi.202201756
27. Sun, Y.; Xia, Y. Shape-controlled synthesis of gold and silver nanoparticles. Science 2002, 298, 2176–2179. https://doi.org/10.1126/science.1077229
28. Liu, Y.; Wang, D. Green synthesis of nanomaterials using polyol methods: recent advances and future perspectives. Green Chem. 2022, 24, 3487–3511. https://doi.org/10.1039/d2gc00568a
29. Wang, A.; Zhang, T. Magnetic nanoparticles as sustainable catalysts in organic synthesis. Curr. Opin. Green Sustainable Chem. 2022, 35, 100613. https://doi.org/10.1016/j.cogsc.2022.100613
30. Liu, P.; Wang, T. Recent progress in the design of magnetically recoverable catalysts for sustainable chemistry. Coord. Chem. Rev. 2023, 474, 214826. https://doi.org/10.1016/j.ccr.2022.214826
31. Zhang, H.; Liu, Y. Synergistic effects in multi-component nanocatalysts for enhanced catalytic performance. Adv. Mater. 2022, 34, 2107425. https://doi.org/10.1002/adma.202107425
32. Li, X.; Wang, Y. Design of multi-layered core–shell nanoparticles for advanced catalytic applications. Nano Today 2022, 43, 101432. https://doi.org/10.1016/j.nantod.2022.101432
33. Goya, G. F.; Berquó, T. S.; Fonseca, F. C.; Morales, M. P. Static and dynamic magnetic properties of spherical magnetite nanoparticles. J. Appl. Phys. 2003, 94, 3520–3528. https://doi.org/10.1063/1.1599959
34. Kodama, R. H. Magnetic nanoparticles. J. Magn. Magn. Mater. 1999, 200, 359–372. https://doi.org/10.1016/S0304-8853(99)00339-9
35. Lu, Y.; Yin, Y.; Mayers, B. T.; Xia, Y. Modifying the Surface Properties of Superparamagnetic Iron Oxide Nanoparticles through A Sol–Gel Approach. Nano Lett. 2002, 2, 183–186. https://doi.org/10.1021/nl015681q